Stretch Dependent Electronic Structure and Vibrational Energy of the Bipyridine Single Molecule Junction

Journal:	*Physical Chemistry Chemical Physics*
Manuscript ID	CP-ART-03-2019-001442.R1
Article Type:	Paper
Date Submitted by the Author:	14-May-2019
Complete List of Authors:	Kobayashi, Shuji; Tokyo Institute of Technology, Department of Chemistry Kaneko, Satoshi; Tokyo Institute of Technology, Chemistry Fujii, Shintaro; Tokyo Inst. of Tech., Chemistry Nishino, Tomoaki; Tokyo Institute of Technology, Department of Chemistry Tsukagoshi, Kazuhito; NIMS, MANA Kiguchi, Manabu; Tokyo Institute of Technology, Department of Chemistry

ARTICLE

Stretch Dependent Electronic Structure and Vibrational Energy of the Bipyridine Single Molecule Junction

Received 00th January 20xx,
Accepted 00th January 20xx

DOI: 10.1039/x0xx00000x

S. Kobayashi [a], S. Kaneko [a], S. Fujii [a], T. Nishino [a], K. Tsukagoshi [b] and M. Kiguchi [a] *

We have studied the stretch dependence of the electronic structure and vibrational energy for the 4,4'-bipyridine (BPY) single molecule junction, which was fabricated by the mechanically controllable break junction (MCBJ) using the highly stable nano MCBJ electrodes. The electronic structure and vibrational energy of the single molecule junction were studied by the current-voltage (*I-V*) curve and surface enhanced Raman scattering (SERS), respectively. The simultaneous SERS and *I-V* curve measurements revealed the lowest unoccupied molecular orbital (LUMO) and vibrational energy of the C-C stretching mode decreased with an increase in the metal-molecule distance. The molecular orbital energy shift and vibrational energy shift can be explained by the change in the degree of the hybridization of molecular and metal orbitals.

Introduction

Molecular adsorption plays an important role in many fields, including catalyst, sensor, organic devices, and so on[1]. In the case of the chemisorption, the molecular and metal orbitals hybridize to form a chemical bond between the molecule and metal, and electrons can transfer between them. The orbital hybridization and electron transfer between the molecule and metal cause the change in the electronic structure of the molecule and the strength of the intramolecular bond. The degree of the hybridization depends on the metal-molecule distance, and the molecular orbital energy changes with the distance. Theoretical calculation have investigated the molecular orbital energy shift in the molecular adsorption process, however, there is little experimental study on the molecular orbital energy shift, due to the experimental difficulty in controlling the metal-molecule distance.

Here, we focus on the single molecule junction, where a single molecule bridges metal electrodes[2]. In the single molecule junction, the metal-molecule distance can be changed by controlling the distance between metal electrodes. The change in the electrical conductance of the single molecule junction has been monitored during the stretching process of the single molecule junction[3, 4]. The single molecular resistive switches have been realized based on the mechanical control of the metal-molecule distance[5, 6].

In order to study intramolecular bonds, the vibrational spectroscopy is an ideal technique[7]. In the case of the single molecule junction, a single molecule is trapped in a metal nano gap, and thus, the single molecule junction is a suitable system for the surface enhanced Raman scattering (SERS)[8, 9]. Recently, we have succeeded in the simultaneous measurement of SERS and conductance, which enabled us to determine the conductance of the well-defined single molecule junction[10]. The electronic structure of the single molecule can be investigated by the current-voltage response (*I-V*)[11, 12]. The electronic coupling between the metal and molecule, and the energy difference between the conduction orbital and Fermi level can be obtained by the *I-V* curve.

In this study, we have measured the SERS and *I-V* curves for a single molecule junction, while the distance between metal electrodes was gradually changed without breaking the junction. The change in the electronic structure and intramolecular bond were observed as a function of the stretch distance. To avoid breaking junctions, a high stability of the single molecule junction is critically important. We have, thus, fabricated the single molecule junction with the mechanically controllable break junction (MCBJ) method using a nano MCBJ electrode. The stability of the junction depends on the length of the free standing bridge of the MCBJ electrode. By using the nano fabrication technique, the size of the free standing bridge was decreased to μm (10^{-6} m) order. In this study, the target molecule is 4,4'-bipyridine (BPY), whose SERS and electric properties have been extensively investigated. We have revealed that the energy of the lowest unoccupied molecular orbital (LUMO) and vibrational energy of the C-C stretching mode decreased with the increase in the metal-molecule distance.

Experimental

The nano MCBJ electrodes were fabricated through a series of standard nanofabrication techniques[13]. A 1 μm thick insulating SiO_2 film was deposited on the polished phosphor bronze substrate (thickness: 0.5 mm) with sputtering. The SiO_2 layer

[a] *Department of Chemistry, Tokyo Institute of Technology, 2-12-1 W4-10 Ookayama, Meguro-ku, 152-8551 Tokyo, Japan.*
E-mail: kiguti@chem.titech.ac.jp

† Electronic Supplementary Information (ESI) available: Evaluation of the gap distance using blank nanogap. See DOI: 10.1039/x0xx00000x

[b] International Center for Materials Nanoarchitectonics (WPI-MANA),, *National Institute for Materials Science, Tsukuba, Ibaraki 305-0044, Japan*

limits the intensity of the Raman background scattering and provides electrical insulation. A polyimide film was deposited on the SiO_2 layer with spin-coating. The nanosized Au electrode (the narrowest constriction: 300 nm×150 nm) was prepared on the substrate by electron beam lithography and lift-off processing. The Cr and Au films (3.5 nm/130 nm) were thermally deposited on the substrate. Subsequently, the polyimide underneath the Au electrode was removed by isotropic reactive ion etching using O_2 plasma (80 W). A free standing Au nano bridge (length: 2 μm) was fabricated on the substrate. The nano MCBJ electrode was mounted on a custom made MCBJ system, consisting of a stacked piezo-element (NEC tokin) and two fixed counter supports (Fig. 1a). The MCBJ setup itself acts as a reduction gear for the motion of the piezo-element (δx) with respect to the relative displacement of the two electrodes (δy). The displacement ratio (r) between δy and δx is given by $r = \delta y/\delta x = 3tu/l^2$, where t, u and l are thickness of the substrate, a free-standing Au nano bridge, and the distance between the two counter supports, respectively. The displacement ratio was 1.5 × 10^{-5} for the present setup, with l=15 mm, t=0.55 mm, u=2 µm (Supporting Information, Fig. S1).

The BPY molecules were adsorbed on the unbroken Au nano bridge using self-assembly from 1mM BPY ethanol solution. The Au nano bridge was stretched and eventually broken by gradually bending the substrate using a piezoelectric push-rod. All measurements were performed at room temperature in air.

The electrical measurements were performed with a Keithley 428 programmable amplifier. The SERS signals were collected using a NanoFinder30 Raman microprobe (Tokyo Instruments) with a near-infrared laser (λ_{ex} = 785 nm) as an excitation light. The laser beam was focused onto the junction using an objective lens with 50× magnification and 0.50 numerical aperture. The laser spot diameter was ~1 μm. The incident light was polarized parallel to the junction axis. The Raman shift was calibrated using Si substrate (520cm^{-1}). The vibrational energy was obtained from the peak position of the vibrational mode in Raman spectra. The standard deviation of the peak position is 0.1cm^{-1} for the Si substrate.

The repeated cycles of SERS and *I-V* curve measurements were performed as the following. First, the Raman spectrum was measured for 1 sec while the piezoelectric push-rod was hold in position. During the Raman measurement, the bias voltage was swept from +1 V to -1V within 2.5 ms to get the *I-V* curve. The *I-V* curves were measured for 20 times. Then, the junction was stretched by 8.5 pm (10^{-12} m), and then Raman spectrum was measured again. The total stretch length was 50pm and total measurement time was 140 sec for each sample. The experiments were performed for 19 distinct samples.

Result and Discussion

Figure 1c shows the Raman image of the nano MCBJ electrode at 1607 cm^{-1}. The intensity of the Raman signal was strongly enhanced only at the gap regime. The Raman signal was sensitive to the polarization direction of the laser light. Polarization parallel to the junction axis resulted in the most intense Raman signal at the gap. These results indicated that the Raman signal was due to the localized surface plasmon excitation of the Au nano electrodes.

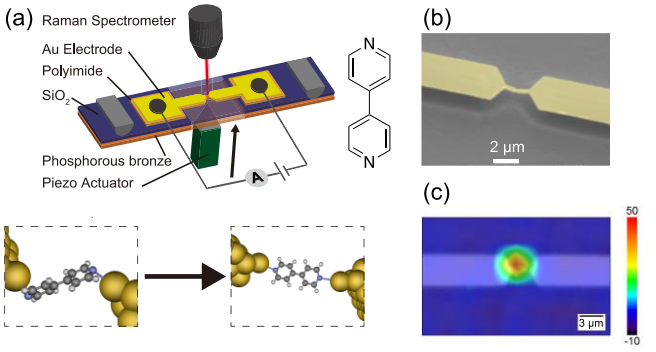

Fig. 1 (a) Experimental setup for simultaneous SERS and *I-V* curve measurement. Inset: Molecular strcuture of 4,4'-bipyridine (BPY) (b) SEM image of the nano MCBJ electrode. (c) Raman image of the nano MCBJ electrode at 1607 cm^{-1}. The photo image of the nano MCBJ electrode is overlapped.

Figure 2 shows the example of the SERS and *I-V* curve of the BPY single molecule junction whose junction conductance was 7.1×10^{-3} G_0 (2e2/h). The SERS spectrum showed clear peaks at 1007 cm^{-1} and 1600 cm^{-1}. These peaks were assigned to the ring breathing mode (υ_1) and C-C stretching mode (υ_{8a}) based on the Raman spectrum of bulk sample. [14] The non-linear *I-V* curve was observed for the BPY single molecule junction. In single level tunnelling model, the transmission probability as a function of incident energy $\tau(E)$ is represented given by

$$\tau(E) = \frac{\Gamma^2}{\Gamma^2+(E-\epsilon)^2} \quad (1)$$

where ε is the energy difference between the conduction orbital (HOMO or LUMO) and the Fermi level, and Γ is the electronic coupling between the molecule and metal electrode. [9, 11, 12] Integration of the transmission probability within an energy window given by the chemical potentials of the electrodes results in an analytical expression for the *I-V* curve of the single molecule junction given by

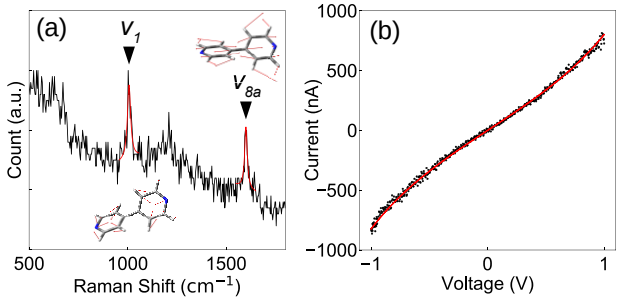

Fig. 2 Typical example of (a) SERS and (b) *I-V* curve of BPY single molecule junction with the fitting result (red curve). Inset: Schematic image of the vibrational mode of υ_1 and υ_{8a} modes.

$$I(V) = \frac{2e}{h}\Gamma\left\{\tan^{-1}\left(\frac{eV-2\epsilon}{2\Gamma}\right) + \tan^{-1}\left(\frac{eV+2\epsilon}{2\Gamma}\right)\right\} \quad (2)$$

The ε and Γ could be obtained by fitting the measured *I-V* curve to equation (2). The obtained values were ε=1.08eV, Γ=0.10eV for the *I-V* curve shown in Fig. 2b. The previously reported thermopower measurement shows that conduction orbital is the LUMO in the case of the BPY single molecule junction[16]. The obtained energy difference was the energy difference between the LUMO and Fermi level.

We then investigate the stretch length dependent SERS and *I-V* curves of the BPY single molecule junction. Figure 3 shows one of the examples during the stretching process. The conductance gradually decreased with increasing stretch length (Fig. 3a). Here, we defined the BPY single molecule junction showing conductance between 0.03 G_0 to 0.001 G_0, based on the previously reported study[5, 15]. The origin of the stretch length was defined as the point where the junction conductance was 0.001 G_0, that is, breaking point of the junction. The vibrational energy of υ_{8a} mode decreased in stretched geometry, while the vibrational energy of the υ_1 mode did not change.

Figure 4 shows the stretch length dependent SERS and *I-V* curves obtained from the 19 samples. The origin was defined as the point where the conductance was 0.001 G_0, and the stretch length was the relative distance from the origin. By stretching the junction by 42pm, the conductance decreased from 0.024 G_0 to 0.001 G_0, and the electronic coupling decreased from 0.16 eV to 0.06 eV. The orbital energy has not change between -40 pm and -20 pm, and then suddenly decreased by 0.2 eV between -20 pm and 0 pm. The vibrational energy of the υ_{8a} mode decreased from 1603 cm^{-1} to 1600 cm^{-1}, while the vibrational energy of the υ_1 mode did not change within 1 cm^{-1}.

We then discuss the change in electronic coupling (Γ), energy difference, and vibrational energy of the υ_{8a} and υ_1 modes for the BPY single molecule junction during the stretching process. The change in the conductance follows the same trend of that of the electronic coupling, suggesting that the change in the conductance was mainly caused by the change in the electronic coupling. It is expected that the electronic coupling between metal and molecular orbital decreases in stretched geometry, which causes the decrease in the conductance. We then focus on energy difference (ε). When a metal and molecular orbital interact, bonding and antibonding orbitals are formed by the orbital hybridization. With a decrease in the metal-molecule distance, the stronger interaction results in increased energy splitting from the original level. In the present study, with an increase in the stretch length, the strength of the metal-molecule interaction decreased. Thus, the stabilization and destabilization energy decreased. Therefore, the hybridized orbital approached to the original molecular and metal orbital, which means the decrease in energy difference.

We then focus on the vibrational energy of υ_{8a} and υ_1 modes. Here, the experimental results are discussed based on the previously reported results for the pyridine molecule having a similar molecular backbone[17-20]. The υ_{8a} and υ_1 modes of pyridine are assigned to similar vibrational modes of BPY. As for the pyridine on the metal surface, larger energy shift of the υ_{8a} mode is reported, which agrees with the present study. It is well known that the υ_{8a} mode is sensitive to the molecular adsorption site, and the υ_{8a} mode has been utilized as a maker of the molecular adsorption[21]. The vibrational energy of the υ_{8a} mode has been calculated for the isolated molecule and the molecule adsorbed on metals [22, 23]. The vibrational energy of the υ_{8a} mode increases with the interaction with the metal atoms.

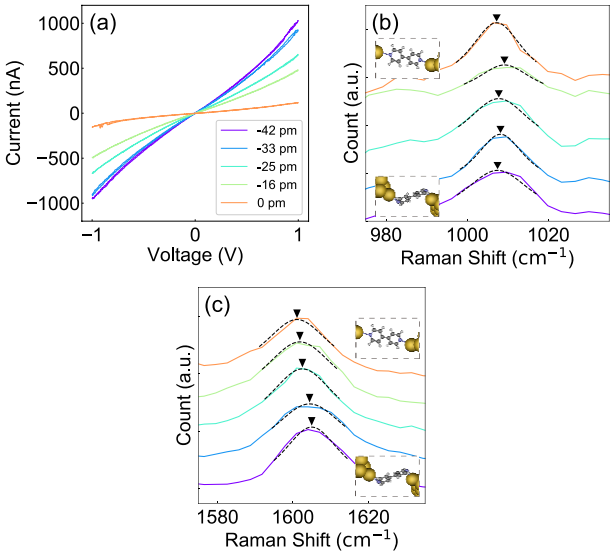

Fig. 3 (a) *I-V* curves and (b) SERS at υ_1 mode and (c) υ_{8a} mode regime for identical BPY single molecule junction during the stretching process. The origin was defined as the point where the conductance was 0.001 G_0, and the stretch length was the relative distance from the origin.

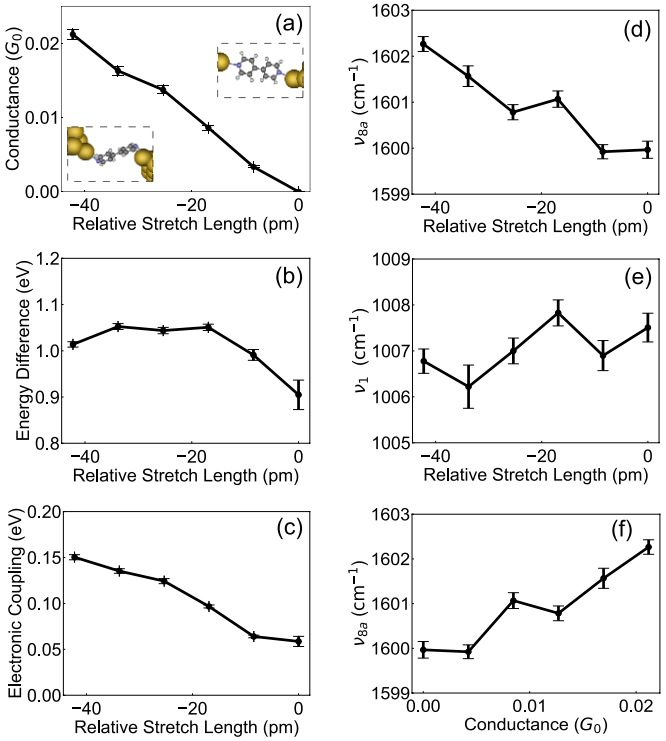

Fig. 4 (a) Electrical conductance, (b) Energy difference between the conduction orbital and Fermi level, (c) Electronic coupling between the molecule and the metal electrode, Wavenumber of (d) υ_{8a} and (e) υ_1 mode during the stretching process of the BPY single molecule junction. The results were obtained from 19 distinct samples. (f) The wavenumber of υ_{8a} plotted versus electrical conductance.

In the present study, the vibrational energy decreased with increasing stretch length. At small metal-molecule distance, the molecule significantly interacts with the metal. By stretching the junction, the strength of the interaction between molecule and metal decreases, and the condition of the molecule approaches to a free molecule, leading to the decrease in the vibrational energy. We can experimentally observe the shift in the molecular energy and vibrational energy as a function of the metal-molecule distance by investigating the single molecule junction, where the metal-molecule distance can be controlled by changing the distance between metal electrodes.

Conclusions

We have experimentally measured the shift in the conducting orbital energy and vibrational energy as a function of the metal-molecule distance by simultaneous SERS and I-V curve measurements using the single molecule junction. The energy of the LUMO and vibrational energy of the C-C stretching mode decreased with the increase in the distance between metal electrodes. These change can be experimentally detected by using the single molecule junction, where the metal-molecule distance can be controlled by changing the distance between metal electrodes.

Conflicts of interest

There are no conflicts to declare.

Acknowledgements

This work was financially supported by Grants-in-Aids for Scientific Research (No. 26102013, 17K19100, 18H03896) from the MEXT, JST CREST (JPMJCR18I4) and TEPCO memorial, and research foundation for opt-science and technology.

Notes and references

1 A. Zangwill, *Physics of surfaces*, Cambridge University Press, Cambrige, England, 1988.
2 Y. Komoto, S. Fujii, M. Iwane and M. Kiguchi, *J. Mater. Chem. C*, 2016, **4**, 8842-8858.
3 M. Kiguchi, O. Tal, S. Wohlthat, F. Pauly, M. Krieger, D. Djukic, J. C. Cuevas and J. M. van Ruitenbeek, *Phys. Rev. Lett.*, 2008, **101**, 046801.
4 C. Bruot, J. Hihath and N. Tao, *Nat. Nanotechnol.*, 2011, **7**, 35-40.
5 S. Y. Quek, M. Kamenetska, M. L. Steigerwald, H. J. Choi, S. G. Louie, M. S. Hybertsen, J. B. Neaton and L. Venkataraman, *Nat. Nanotechnol.*, 2009, **4**, 230-234.
6 M. Kiguchi, T. Ohto, S. Fujii, K. Sugiyasu, S. Nakajima, M. Takeuchi and H. Nakamura, *J. Am. Chem. Soc.*, 2014, **136**, 7327-7332.
7 R. H. Smit, Y. Noat, C. Untiedt, N. D. Lang, M. C. van Hemert and J. M. van Ruitenbeek, *Nature*, 2002, **419**, 906-909.
8 S. Nie and S. R. Emory, *Science*, 1997, **275**, 1102-1106.
9 Z. Ioffe, T. Shamai, A. Ophir, G. Noy, I. Yutsis, K. Kfir, O. Cheshnovsky and Y. Selzer, *Nat. Nanotechnol.*, 2008, **3**, 727-732.
10 S. Kaneko, D. Murai, S. Marques-Gonzalez, H. Nakamura, Y. Komoto, S. Fujii, T. Nishino, K. Ikeda, K. Tsukagoshi and M. Kiguchi, *J. Am. Chem. Soc.*, 2016, **138**, 1294-1300.
11 Y. Kim, T. Pietsch, A. Erbe, W. Belzig and E. Scheer, *Nano Lett.*, 2011, **11**, 3734-3738.
12 Y. Isshiki, S. Fujii, T. Nishino and M. Kiguchi, *J. Am. Chem. Soc.*, 2018, **140**, 3760-3767.
13 S. Kobayashi, S. Kaneko, S. Fujii, T. Nishino, M. Kiguchi and K. Tsukagoshi, *eJSSNT*, 2018, **16**, 145-149.
14 S.-W. Joo, *Vib.Spectrosc.*, 2004, **34**, 269-272.
15 B. Xu and N. J. Tao, *Science*, 2003, **301**, 1221-1223.
16 T. Kim, P. Darancet, J. R. Widawsky, M. Kotiuga, S. Y. Quek, J. B. Neaton and L. Venkataraman, *Nano Lett.*, 2014, **14**, 794-798.
17 C. Zuo and P. W. Jagodzinski, *J. Phys. Chem. B.*, 2005, **109**, 1788-1793.
18 L. Jensen, L. L. Zhao and G. C. Schatz, *J. Phys. Chem. C*, 2007, **111**, 4756-4764.
19 L. Zhao, L. Jensen and G. C. Schatz, *J. Am. Chem. Soc.*, 2006, **128**, 2911-2919.
20 J. P. Su, Y. T. Lee, S. Y. Lu and J. S. Lin, *J. Comput. Chem.*, 2013, **34**, 2806-2815.
21 T. Kitano, T. Shishido, K. Teramura and T. Tanaka, *ChemPhysChem*, 2013, **14**, 2560-2569.
22 D.-Y. Wu, S. Duan, B. Ren and Z.-Q. Tian, *J. Raman Spectrosc.*, 2005, **36**, 533-540.
23 Y. Ma, S. Y. Wang, Z. Li, W. Hu, S. Z. Jiang, X. N. Song and C. K. Wang, *J. At. Mol. Sci.*, 2017, **8**, 127-130.

TOC

Change in the molecular orbital energy and vibrational energy of the bipyridine single molecule junction as a function of stretch distance.